

# **CONSTRAINING GAS HYDRATE OCCURRENCE IN THE NORTHERN GULF OF MEXICO CONTINENTAL SLOPE: FINE SCALE ANALYSIS OF GRAIN-SIZE IN HYDRATE-BEARING SEDIMENTS**

**Alexandra Hangsterfer\***  
**Geosciences Research Division**  
**Scripps Institution of Oceanography**  
**9500 Gilman Drive, Mail Code 0208**  
**La Jolla, CA 92093**  
**USA**

**Neal Driscoll and Miriam Kastner**  
**Geosciences Research Division**  
**Scripps Institution of Oceanography**  
**9500 Gilman Drive, Mail Code 0208**  
**La Jolla, CA 92093**  
**USA**

## **ABSTRACT**

Within the subseafloor, methane hydrates form within the gas hydrate stability zone (GHSZ). Two areas within the Gulf of Mexico (GOM) were investigated in this study: Keathley Canyon and Atwater Valley. The GOM contains an underlying petroleum system and deeply buried, yet dynamic salt deposits. Salt tectonics and fluid expulsion upward through the sediment column lead to the formation of fractures, through which high salinity brines migrate into the GHSZ, destabilizing gas hydrates. Originating from the thermal and biogenic degradation of organic matter, thermogenic and biogenic hydrocarbons also migrate to the seafloor along the GOM's northern slope. Gas hydrate occurrence can be controlled by either primary permeability, forming in coarse-grained sediment layers, or by secondary permeability, forming in areas where hydrofracture and faulting generate conduits through which hydrocarbon-saturated fluids flow. The goal of this study is to determine the relationship between grain-size, permeability, and gas hydrate distribution. Grain-size analyses were performed on cores taken from Keathley Canyon and Atwater Valley in the GOM, on sections of cores that both contained and lacked gas hydrate. The initial results indicate that gas hydrate occurrence in Keathley Canyon and Atwater Valley is constrained by secondary permeability, being structurally controlled by hydrofractures and faulting that act as conduits through which methane-rich fluids flow.

*Keywords:* Methane hydrates, Gulf of Mexico, grain-size, permeability, thermal anomaly

## **INTRODUCTION**

Methane hydrates are ice-like solids that contain gaseous methane molecules within their crystalline structures. Methane hydrate formation and distribution is constrained by temperature and

pressure, the availability of methane, and the chlorinity of the surrounding porewater [1]. Particular to the Gulf of Mexico (GOM) is the pervasive occurrence of buried middle Jurassic Louann salt deposits that can influence the

---

\* Corresponding author: Phone: +1 858 534 4716 Fax +1 858 534 7889 E-mail: ahangste@ucsd.edu

occurrence of gas hydrate [2, 3]. Sediment loading, sea-level change and salt tectonics deforms and faults the overlying sediment carapace and thus makes this region of the GOM an active site of fluid expulsion [4]. Resulting fractures associated with salt tectonics range from shallow, meter long faults, to deeply buried growth faults that extend hundreds to thousands of meters into the sediment column [4]. Initially, salt-related faults act as conduits for the migration of deeply buried fluids, including salt brine, and both thermogenic and biogenic gas-containing fluids [5]. Through time, gas hydrate and authigenic carbonate precipitation occurs within the conduits, inhibiting passage of fluids through these permeability pathways. Active salt tectonics in the GOM results in the continual generation of fractures, and, thus, new conduits through which fluids migrate.

Thermogenic methane production results from the thermal degradation of oil and organic matter, while biogenic hydrocarbon gases are produced as a result of biological methanogenesis. Both thermogenic and biogenic methane molecules are incorporated in the gas hydrates structures observed in the GOM [5]. Concurrently, high salinity brines are expelled from the deeply buried salt deposits [2]. It has been determined that gas hydrate occurrence diminishes in regions with high-salinity brines [3], where brines can destabilize gas hydrates and suppress further gas hydrate formation [6].

While still uninhibited by carbonates and brine saturation, fault controlled permeability structures facilitate the migration of gas-containing fluids upward into the GHSZ. As such, salt deformation and secondary permeability might help explain the occurrence of gas hydrate structures in the sediment column where temperature and pressure conditions are conducive for stable hydrate occurrence.

The principal goal of this study is to determine the relationship between grain-size, permeability, and gas distribution. To accomplish this, we examined the grain-size distribution of hydrate-bearing sediments in Atwater Valley and Keathley Canyon in the GOM (Figure 1). Given the predominance of fine-grained sediment in the GOM, our initial hypothesis is that gas hydrate distribution is related to fault-controlled, secondary permeability. Consequently, primary permeability is not the controlling factor in hydrate distribution within the sites examined in the GOM.

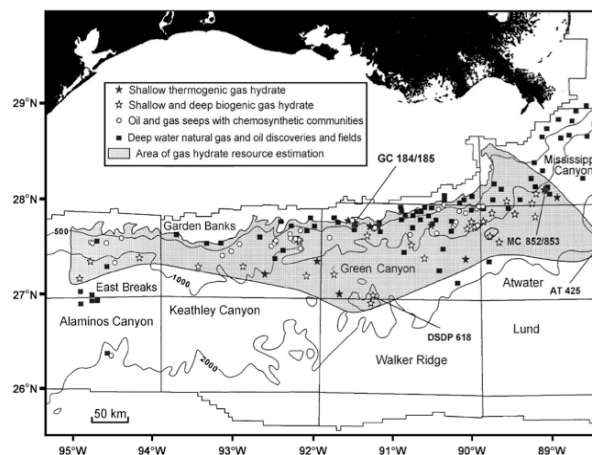


Figure 1 Location of petroleum fields, hydrocarbon seeps, gas hydrate occurrence, and the area of gas hydrate boundaries in the northwestern GOM continental slope [5].

## METHODS

### Determination of hydrate occurrence

Gas hydrate dissociation is an endothermic reaction that reduces the temperature of adjacent sediments. Therefore, temperature is used as a proxy for hydrate occurrence in cores that have been recovered from the seafloor environment. Core sections containing a negative thermal anomaly are characterized as hydrate-bearing sediments [7,8].

The cores recovered from the Gulf of Mexico Hydrate Joint Industry Project (GOM/JIP) cruise in May 2005 onboard the drilling vessel *Uncle John*, are stored at the Geological Collections at Scripps Institution of Oceanography (SIO). 5,540ft of sediment was recovered from seven wells from both Atwater Valley and Keathley Canyon (Detailed list of cores included in Table 1).

Location and Site	Depth (mbsf)
AT 13 #1	246.6
AT 14 #1	286.8
<b>AT 13 #2</b>	<b>200.0</b>
ATM 1	24.4
<b>ATM 2</b>	<b>31.4</b>
KC 151 #2	459.0
<b>KC 151 #3</b>	<b>440.4</b>

Table 1. Total depth drilled for each site. KC=Keathley Canyon; AT = Atwater Valley; ATM= Atwater Valley mound sites. Bold print indicates sites investigated in this study.

Using thermal anomalies as proxies for the occurrence of methane hydrate within the cores, sediment was sampled and the grain-size distributions were measured to determine if there is a correlation between gas hydrate distribution and grain-size.

### **Core Analysis**

Upon recovery, cores were imaged with both a track-mounted and a hand-held infrared (IR) camera [9]. Processing of the IR images resulted in the generation of down-core temperature profiles using the ThermoCam Researcher software (FLIR Systems). Sampling for porewater, to be analyzed for dissolved inorganic geochemical constituents, were based on occurrence of negative thermal anomalies in the IR images. Porewater samples were taken at regular intervals in each core recovered from all sites (Table 2). Background porewater samples were taken adjacent to prominent IR-detected thermal anomalies (Table 2).

Core sections removed for chemical analysis were extruded from the core liner, scraped clean to remove sediment possibly contaminated by seawater (drilling fluid), and placed in a pressurized titanium squeezer, extracting the porewater from the sediment. The remaining, flattened sediment section from which porewater had been squeezed, is termed "squeezecake". Squeezecakes taken from sections of the core that were adjacent to IR-detected thermal anomalies were targeted for grain-size analysis. Background samples were taken from areas with no IR-detected thermal anomaly.

Grain-size distribution for each sample was determined using a two-step process: 1) samples were wet sieved to separate the coarse ( $>63\mu\text{m}$ ) and fine ( $<63\mu\text{m}$ ) fractions and 2) then a Coulter Counter was used to determine the grain-size distribution of sediment particles within the fine-fraction. The grain-size analysis methods used were modified from [10].

### **Targeting core sections to sample**

Nine core sections, exhibiting minimal deformation and consistent recovery, were targeted for grain-size analysis from three sites: Keathley Canyon (151-3), Atwater Valley (13-2) and Atwater Valley Mound Site 2. Five of the core sections displayed strong negative thermal anomalies.

## **RESULTS**

Presented here are the data from three representative cores: two are hydrate-bearing samples, and one is a background sample. (Figures 2, 3 and 4).

When sediments taken from a squeezecake were analyzed, sediments samples were also taken from areas of the remaining core that were immediately above and below the squeezecake sediment. This was done to ensure that the sediments exhibiting a negative thermal anomaly were sampled continuously through the depth where the temperature returned to background values.

Data gaps shown in the figures are locations where shipboard samples were removed for other analyses, and thus these intervals were unavailable for grain-size analysis.

### **KC 151-3 Core 15C**

A pronounced temperature anomaly observed in core KC (Keathley Canyon) 151-3 section 15C (Figure 2) at approximately 253.5 mbsf exhibits a  $2.0^{\circ}\text{C}$  anomaly that corresponds to a visually distinct cold section (dark purple in color) within the IR image. Examination of the grain-size shows little to no variability in this core. Within the squeezecake, an average grain-size is reported because it is difficult to determine exact depth within the core. Within the hydrate-bearing core, coarse-grained percentages vary only slightly between 0.4% and 1.7%. The highest coarse-grained percentage corresponds to the sampled squeezecake sediment, which does not correspond with the section of the core containing a prominent temperature anomaly. It is also observed that the lowest coarse-grained percentages do not correspond to sections of the core characterized by a thermal anomaly. There is no systematic relationship between the occurrence of coarser-grained sediment sections and temperature anomalies in this core.

Fine-grained sediments make up the highest percentage within core 151-3 section 15C, fluctuating between 98.3% and 99.6%. The lowest fine-grained percentage was recorded within a squeezecake at a depth of approximately 253.5 mbsf, void of a negative thermal anomaly. Within the fine-grained fraction, the majority of sediment particles, between 66.4% and 85.2%, fell within the clay size-fraction ( $4-1\mu\text{m}$ ). Between 2.7% and 19.5% of fine particles fell within the silt size-fraction ( $63-4\mu\text{m}$ ), while 2.8% to 16.1% of fine-

grained particles were less than 1µm in diameter. Within the fine fraction, the size distribution of sediment particles did not correspond to the presence of thermal anomalies, varying inconsistently with temperature fluctuations.

**Pore Fluids Subsampling Plan At Each Site:**

<b>1<sup>st</sup> Core</b>	Excise a 10-15 cm whole round from the bottom of every section.
<b>2<sup>nd</sup> Core</b>	Excise a 10-15 cm whole round from the bottom of every 2 <sup>nd</sup> section.
<b>3<sup>rd</sup> Core</b>	Excise a 15-20 cm whole round from the bottom of every 1 <sup>st</sup> and 4 <sup>th</sup> (or 2 <sup>nd</sup> and 5 <sup>th</sup> ) section for 5 meter-long cores. Excise a 15-20 cm whole round from the bottom of every 1 <sup>st</sup> , 4 <sup>th</sup> and 7 <sup>th</sup> sections for 8 meter-long cores.
<b>4<sup>th</sup> and following cores</b>	Excise a 15-30 cm whole round from the bottom of every 3 <sup>rd</sup> section for 5 meter-long cores; except when in estimated BSR depth range, in which case, at the bottom of the 2 <sup>nd</sup> and 4 <sup>th</sup> sections. Excise a 15-30 cm whole round from the bottom of every 2 <sup>nd</sup> and 6 <sup>th</sup> sections for 8 meter-long cores

**Additional Subsamples taken from Each Site:**

<b>Adjacent to prominent IR-detected gas hydrates</b>	Excise 10-20 cm whole rounds adjacent to IR detected gas hydrate, with a maximum of one per core.
<b>Gas Hydrates (To be sub-sampled for gas analysis)</b>	Remove a 3-5 cc (larger if possible) sample for water analysis Wrap gas hydrate sample in aluminum foil and cotton bag that has been labeled. Store in liquid N <sub>2</sub> dewar.

Table 2.

**AT 13-2 Core 13H**

Core AT (Atwater Valley) 13-2 section 13H (Figure 3) does not show a marked temperature deviation, with only a slight fluctuation between 18.9°C and 21.2°C. Also, section 13H does not have a marked visual anomaly in the corresponding IR image. Grain-size distribution within this core varies only slightly, with a coarse-grained percentage fluctuating between 2.2% and 4.0%. Fine-grain percentages range between

96.0% and 99.3%, with silt particles varying significantly between 2.6% and 45.8%, clay particles ranging between 47.8% and 86.4%, and particles less than 1µm ranging between 0.0% and 10.0%. The slight cooling seen down-core through the sampled interval corresponds to a statistically insignificant decrease in coarse-grained and increase in fine-grained percentages. The silt and clay percentages vary inversely, with no considerable relation to the slight decline that is observed in the temperature. No major trends are observed in the grain size distribution within core AT 13-2 section 13H.

**KC 151-3 Core 15C (252.51-254.01mbsf)  
Hydrate-Bearing/Thermal Anomaly**

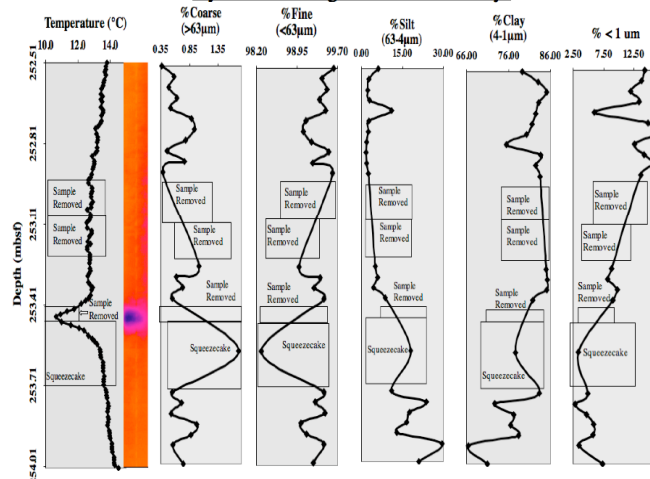


Figure 2 Gas hydrate-containing core (15C) from Keathley Canyon site 151-3.

**AT 13-2 Core 13H (142.37-143.51mbsf)  
No Hydrate/No Thermal Anomaly**

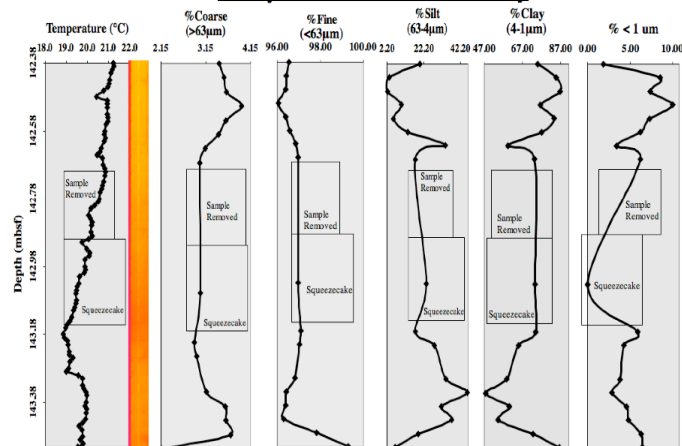


Figure 3 Background core (13H) from Atwater Valley site 13-2.

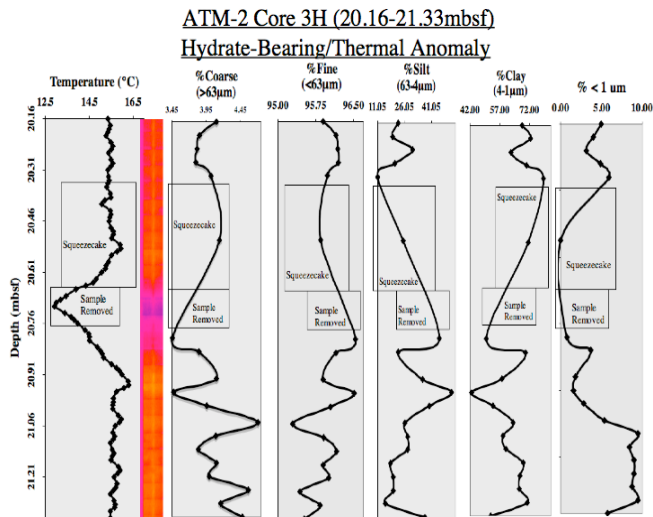


Figure 4 Gas hydrate-containing core (3H) from Atwater Valley Mound site 2.

### ATM 2 Core 3H

Core ATM (Atwater Valley Mound) 2 section 3H (Figure 4) contains a thermal anomaly, at approximately 20.7 mbsf, where the temperature drops from approximately 15.5°C to approximately 13.0 °C. The temperature excursion corresponds to a marked dark purple colored cold section seen in the IR image. Examination of the grain-size for this core shows variability down-core, but with only a slight change in the percentage of each grain-size fraction. For example, the coarse-grained fraction varies only between 3.5% and 4.7%, while the fine-grained varies between 95.3% and 96.5%. The section of the core that corresponds to the negative thermal anomaly had been previously removed for other analysis. Within the sampled squeezecake, which encompasses only a small section of core that is characterized as part of the negative thermal anomaly, there is no significant change in the coarse- or fine-grained percentage. The section of the core that contains the most variation within the coarse- and fine-grained fractions (20.8-21.3 mbsf) corresponds to constant temperatures (approximately 15.5 °C) within the same depth range.

Within the fine-grained fraction, there is a much more significant variation in the percentages of silt, clay, and particles less than 1 µm in diameter. Silt percentages range from 11.0% and 52.2%, clay percentages range from 42.7% and 79.0%, and the percentage less than 1 µm ranges

from 0.0% to 9.3%. The silt and clay profiles vary inversely, while the clay and percentage less than 1 µm vary consistently. The silt profile exhibits a similar down-core trend when compared to the fine-grained profile down-core, while the clay and percentage less than 1 µm profiles exhibit a similar down-core trend when compared to the coarse-grained profile (Figure 4). Within the silt profile for ATM 2 section 3H, there is only one depth (21.0 mbsf) at which the silt percentage reaches a value greater than 50.0%. Throughout the rest of the core section, the clay percentages are greater than 50.0%, making the majority of the fine-grained fraction composed of clay particles.

Although the section of the core that corresponds most closely to the negative temperature anomaly had been removed and the grain size could not be analyzed, it appears that there exists a decreasing trend in the coarse-grained profile as the temperature decreases, starting in the sampled squeezecake sediments (Figure 4). Although the fine-grained fraction percentage increases as a result, within the fine-fraction, the percentage of silt particles increases from 11.0% and 45.5%, as the coarse-grained percentage decreases from 4.0% and 3.5% within a depth range of 20.3 mbsf and 20.8 mbsf. This is the only inferred trend within the thermal anomaly-containing core section taken from the Atwater Valley Mound site.

Consistent with the two other core sections that are presented here, one that contains and one that lacks a thermal anomaly, this core section is predominantly composed of fine-grained sediment particles and lacks a definable trend linking the down-core variation in grain-size and temperature fluctuations.

### DISCUSSION AND CONCLUSIONS

The grain-size analysis indicates that there is no discernable relationship between the occurrence of coarse-grained sediment horizons and the distribution of gas hydrates in Keathley Canyon, Atwater Valley, or the Atwater Valley mound site. This is distinctly different than the documented link between hydrate distribution and the presence of sand layers in Southern Hydrate Ridge [8]. The sampled sites are characterized as being predominantly fine-grained, composed of mostly clay-sized particles (Figures 2, 3 and 4), regardless of whether or not the core contained or

lacked gas hydrate. Gas hydrates are thus forming in low-permeability sediments successfully, providing evidence that primary permeability does not necessarily control the occurrence of gas hydrates in the sampled sites in the GOM. Therefore, it is initially concluded that gas hydrate distribution within the sampled regions of the GOM is constrained by secondary fault-controlled permeability.

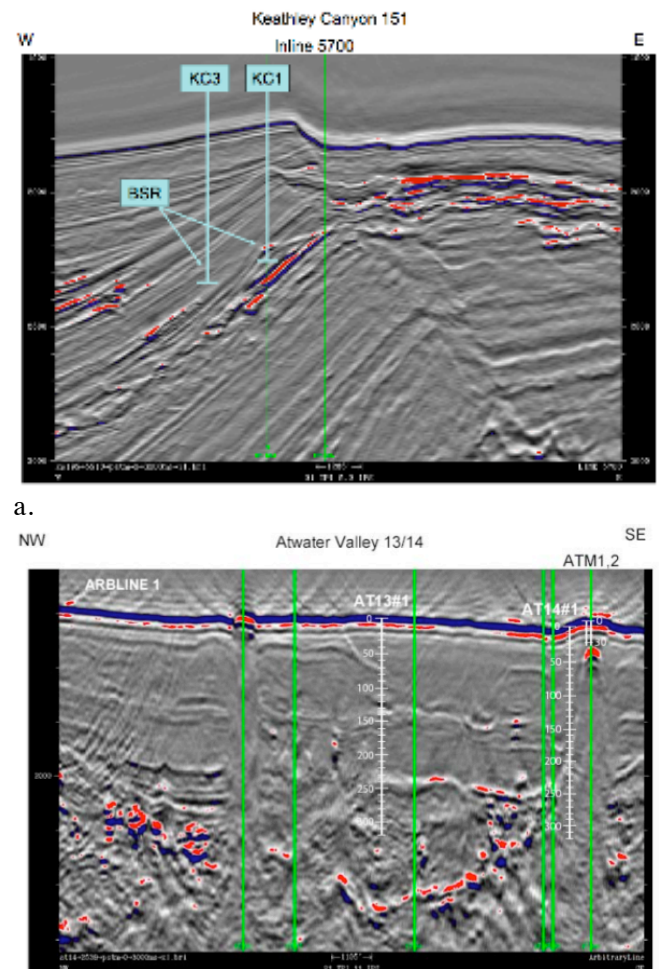
It has previously been concluded that the alkalinity and sulfate gradients are controlled mostly by the upward flux of methane to the seafloor [11]. The anaerobic oxidation of methane (AOM) is an important driving force of sulfate reduction in the shallow region of the sediment column in Keathley Canyon. Concurrently, some of the alkalinity produced is being removed by the precipitation of authigenic carbonate in the deeper region of the sediment column [11]. Both the Atwater Valley mound site and Keathley Canyon exhibit high salinity values, up to 56 ppt, resulting from the migration of diagenetically altered, high-salinity brine flowing upward through sediment column [11].

Development of various fracture types results from post-depositional alteration in the sediment column, constraining the permeability controlled migration of subseafloor fluids in the GOM. Movement of deeply buried salt sheets initiates fracturing in the sediment that form growth faults that can grow thousands of meters throughout the sediment column. Shallow salt movement forms much smaller fractures that extend only meters in the upper sediment column [4]. Hydrofractures may also play a role in forming conduits through which methane-rich fluids flow. Hydrofractures are likely formed when the pressure gradient generated by the massive quantity of deeply buried salt brine and hydrocarbon-bearing fluids exceeds the strength of the overlying sedimentary layers.

Seismic images acquired in Keathley Canyon and Atwater Valley (Figure 5) reveal intense fluid expulsion at the subseafloor. The bottom-simulating reflector (BSR) is greatly disrupted as a result of the upward advection of highly saline brines and gas-charged fluids. In particular, methane-charged fluids flow upward through fractures into the GHSZ, saturating the fine-grained sediments there, forming vein-filling gas hydrate within the sediments pore spaces.

Overall, the evidence here supports our hypothesis that gas hydrate occurrence in the

Atwater Valley and Keathley Canyon is a result of secondary permeability, resulting from hydrofracture and faulting, and not as a consequence of lithology-controlled primary permeability.



b. Figure 5 Seismic lines in the Keathley Canyon 151 block. KC1 references the logging while drilling (LWD) hole KC 151 #2, and the coring hole KC 151 #3. KC3 is a reference site that was not drilled. The arrows show the depth of the BSR that is only faintly imaged in this figure [9]. (b) Seismic lines in Atwater 13/14 blocks showing three drilling sites. The white lines indicate the position of the LWD sites (AT 13#2 at same location as AT 13#1, and mound sites ATM1, ATM2) The green lines indicate the positions of drilling locations that were previously proposed [9].

## REFERENCES

[1] Sloan ED, Koh CA. *Clathrate hydrates of natural gases (Third Edition)*. Boca Raton: C.R.C. Press, 2008. p.721.

- [2] Worrall DM, Snelson S. *Evolution of the northern Gulf of Mexico with emphasis on Cenozoic growth faulting and the role of salt*. In: Bally AW, Palmer AR editors. *The geology of North America—An overview*: Boulder, Colorado, Geological Society of America, *Geology of North America*, Volume A, 1989. p. 97–138.
- [3] Sassen R, Sweet ST, DeFreitas DA, Eaker NL, Roberts HH, Zhang C. *Brine vents on the Gulf of Mexico slope: hydrocarbons, carbonate-barite-uranium mineralization, red beds, and life in an extreme environment*. *Gulf Coast Section Society of Economic Paleontologists and Mineralogists* 2004:444-463.
- [4] Roberts HH, Carney R. *Evidence of episodic fluid, gas, and sediment venting on the northern Gulf of Mexico slope*. *Economic Geology* 1997:92:863-879.
- [5] Sassen R, Sweet ST, Milkov AV, DeFreitas DA, Salata GG, McDade EC. *Geology and geochemistry of gas hydrates, central Gulf of Mexico continental slope*. *Trans. Gulf Coast Assoc. Geol. Soc.* 1999:49:462–468.
- [6] Milkov AV, Lee YJ, Borowski WS, Torres ME, Xu W, Tomaru H, Trehu AM, Schultheiss P, Dickens GR, Claypool GE. *Co-existence of gas hydrate, free gas, and brine within the regional gas hydrate stability zone at Hydrate Ridge (Oregon margin): evidence from prolonged degassing of a pressurized core*. *Earth Planet. Sci. Lett.* 2004:222: 829-843.
- [7] Ford KH, Naehr TH, Skilbeck CG and Leg 201 Scientific Party. *The use of infrared thermal imaging to identify gas hydrate in sediment cores*. In: D'Hondt SL, Jørgensen BB, Miller DJ, et al., editors. *Proceedings of the Ocean Drilling Program, Initial Reports 201*. College Station, TX: Ocean Drilling Program, 2003. p. 1-20.
- [8] Weinberger JL, Brown KM, Long PE. *Painting a picture of gas hydrate distribution with thermal images*. *Geophysical Research Letters* 2005:32:L04609.
- [9] Conte A., Bloys B. *Gulf of Mexico Gas Hydrates Joint Industry Project Operational Summary of 2005 Drilling and Coring Program*, Cruise Report: The Gulf of Mexico Gas Hydrate Joint Industry Project 2006. Houston, TX: Chevron Corporation, 2006. See Also: <http://www.netl.doe.gov/technologies/oil-gas/publications/Hydrates/reports/GOMJIPCruise05.pdf>
- [10] Poppe LJ, Elisaon AH, Fredericks JJ, Rendigs RR, Blackwood D, Polloni, CF. *Chapter1: Grain-Size Analysis of Marine Sediments: Methodology and Data Processing*. U.S. Geological Survey Open-File Report 00-358. USGS. 2000. See also: <http://pubs.usgs.gov/of/2000/of00-358/index.htm>
- [11] Kastner M, Claypool G, Robertson GA. *Geochemical constraints on the origin of the pore fluids and gas hydrate distribution at Atwater Valley and Keathley Canyon, northern Gulf of Mexico*. *Marine and Petroleum Geology* 2008: in press.

